




PAPER

[View Article Online](#)
[View Journal](#) | [View Issue](#)Cite this: *J. Mater. Chem. A*, 2019, 7, 4829**Zwitterionic copolymer additive architecture affects membrane performance: fouling resistance and surface rearrangement in saline solutions†**Papatya Kaner, ^a Alexander V. Dudchenko,^b Meagan S. Mauter ^{bc} and Ayse Asatekin ^{*a}

Membrane separations are simple to operate, scalable, versatile, and energy efficient, but their broader use is curtailed by fouling or performance decline due to feed component depositing on the membrane surface. Surface functionalization with groups such as zwitterions can mitigate the adsorption of organic compounds, thus limiting fouling. This can be achieved by using surface-segregating copolymer additives during membrane manufacture, but there is a need for better understanding of how the polymer structure and architecture affect the effectiveness of these additives in improving membrane performance. In this study, we aim to explore the impact of the architecture of zwitterionic copolymer additives for polyvinylidene fluoride (PVDF)-based membranes in fouling mitigation and ionic strength response. We prepared membranes from blends of PVDF with zwitterionic (ZI) copolymers with two different architectures, random and comb-shaped. As the random copolymer, we used poly(methyl methacrylate-*random*-sulfobetaine-2-vinyl pyridine) (PMMA-*r*-SB2VP) synthesized by free radical polymerization. The comb-shaped copolymer was synthesized by grafting SB2VP side-chains from a PVDF backbone by controlled radical polymerization. Membranes were fabricated from PVDF-copolymer blends containing up to 5 wt% ZI copolymer. Compared to the additive-free PVDF membrane, water permeance increased five-fold with 5 wt% addition of either copolymer. The comb copolymer additive led to better resistance to fouling by a saline oil-in-water emulsion and to simulated protein adsorption in Atomic Force Microscopy (AFM) force measurements. The additive architecture had a significant influence on how membranes respond to changes in feed salinity, which is known to affect intra- and inter-molecular interactions in zwitterionic polymers. The random copolymer containing membrane showed a small and mostly reversible decrease in its permeance with salinity. In contrast, the comb copolymer-containing membrane underwent a conformational reorganization in saline solutions that leads to an irreversible permeance decrease, increased zwitterionic group content on the membrane surface, and smoother surface topography. The higher mobility of the zwitterionic groups in the comb-shaped architecture facilitates reorganization of the zwitterionic side-chains in response to ionic strength. Overall, this study establishes a new approach for developing highly fouling resistant membranes and defines how the architecture of a zwitterionic copolymer additive impacts the ionic strength response and fouling resistance of the membrane.

Received 30th November 2018
Accepted 25th January 2019

DOI: 10.1039/c8ta11553b

rsc.li/materials-a

1. Introduction

Membrane separations are green alternatives to other unit operations such as distillation and extraction due to their ease of operation, scalability, versatility and energy efficiency.^{1–4} Yet,

broader use of membranes in many processes is limited by membrane fouling, defined by performance loss due to the adsorption and accumulation of feed components on the membrane surface.^{5,6} Membrane fouling restricts flow through the membrane as a consequence of feed component depositing

^aDepartment of Chemical and Biological Engineering, Tufts University, Medford, MA 02155, USA. E-mail: Ayse.Asatekin@tufts.edu; Fax: +1 617 627 3991; Tel: +1 617 627 4681

^bDepartment of Civil and Environmental Engineering, Carnegie Mellon University, Pittsburgh, PA 15213, USA

^cDepartment of Engineering and Public Policy, Carnegie Mellon University, Pittsburgh, PA 15213, USA

† Electronic supplementary information (ESI) available: Chemical characterization of the PMMA-*r*-SB2VP copolymer, initiation efficiency of chlorine groups in the backbone polymer PVDF-*co*-CTFE during ARGET-ATRP, chemical characterization of the PVDF-*g*-SB2VP copolymer after water wash, membrane morphology, surface hydrophilicity and water permeance, protein rejection by the M-PVDF membrane, calculation of the molecular sizes of the SB2VP monomer and trimer, oil fouling test, AFM detachment force measurements, and dynamic protein fouling test. See DOI: 10.1039/c8ta11553b

on the membrane surface and inside the pores. Fouling poses a major obstacle to broader implementation of membrane technology due to its implications in driving up energy, maintenance, and membrane replacement costs.^{7–9} This has motivated extensive research on understanding and preventing fouling in membrane systems, from the study of the fouling mechanism to the design of fouling resistant membranes.^{8–12}

Membrane fouling occurs through multiple mechanisms, including the adsorption of biomacromolecules (*e.g.* proteins and alginate) and other organic compounds (*e.g.* oil) on the membrane surface, the physical accumulation of particulates forming a cake, and the adhesion and growth of microorganisms. While cake formation is typically managed by module design, controlling the membrane surface chemistry is crucial in mediating both adsorptive fouling by organic compounds and cell adhesion. This can be achieved by functionalizing the membrane surface with chemical moieties that strongly resist organic molecule adsorption and cell adhesion.^{12–15}

One such class of functional groups is zwitterionic moieties. Zwitterions contain equal numbers of anionic and cationic groups, connected by covalent bonds. Zwitterionic groups are found to be highly resistant to the adsorption of proteins and other biomolecules from aqueous solutions^{13,16–18} due to their very high degree of hydration.¹⁹ Zwitterionic groups can be incorporated onto a membrane surface by various methods including surface grafting^{20–27} or coating.^{28–31} These methods, however, involve post-modification of formed membranes by additional manufacturing steps, adding to costs. They also typically cause initial declines in pure water flux.

An efficient method for creating membranes with hydrophilic, fouling-resistant surfaces without added manufacturing steps involves the addition of an amphiphilic surface-segregating copolymer to the commodity polymer commonly used to prepare membranes (*e.g.* PAN and polyvinylidene fluoride (PVDF)). The membrane is then manufactured by non-solvent induced phase separation (NIPS), the current industry standard manufacturing method for commercial ultrafiltration (UF) membranes. This approach has previously been applied to attain membranes with fouling resistant zwitterionic groups on the membrane surface and pore walls using zwitterionic copolymers with random architecture as additives.^{32–40} If the additive is designed so that its hydrophobic segments remain compatible with the commodity polymer throughout the casting process, membranes with exceptional fouling resistance can be obtained.⁴⁰ When used as additives during NIPS, random zwitterionic copolymers only result in either isolated zwitterionic groups or highly constrained short segments on the membrane surface. Other copolymer architectures, such as comb-shaped copolymers, may enable higher mobility of poly-zwitterion chains, which may lead to enhanced fouling resistance through steric effects.^{41,42} Comb-shaped copolymers with a hydrophobic backbone and hydrophilic side-chains also have a proven track record of efficient surface segregation owing to the entropic tendency of chain ends to occupy interfaces.^{41,43–47}

In addition to being fouling resistant, zwitterionic materials are also known to be ionic strength responsive.^{48–52} At increased ionic strengths, the strong dipole–dipole interactions between

the inversely charged co-ions forming the zwitterionic groups diminish as they rather associate with counter-ions from the salt. As a result, the chain expands. At lower ionic strengths, zwitterionic groups form intra- and inter-molecular associations, leading to collapsed chains.^{48,49} This effect, termed the anti-polyelectrolyte effect, can be utilized for developing ionic strength- (or salinity-) responsive membranes. The effect of ionic strength on the performance of membranes that feature zwitterionic groups is strongly dependent on the configuration of zwitterions on the membrane surface. For instance, in grafted zwitterionic systems, membrane flux declines with increasing ionic strength due to expansion of polymeric chains into the membrane pores.^{51–53} On the other hand, polyacrylonitrile (PAN)-based membranes prepared with a zwitterionic random copolymer additive showed improved fouling resistance to proteins at higher ionic strengths, leading to higher flux for protein solutions at higher ionic strengths.³³

Most stimuli-responsive polymers show a reversible response to external stimuli.^{33,54–62} However, hysteretic or irreversible phase transitions have been reported in systems where changes in polymer conformation occur in combination with the formation of inter-chain bonds (*e.g.* hydrogen bonding).^{63–69} For example, phase transitions of the poly(lactic acid-co-glycolic acid)-*g*-poly(ethylene glycol) copolymer in aqueous solutions⁷⁰ and expansion/collapse of poly(*N*-isopropylacrylamide) (PNIPAM) chains in water⁷¹ both exhibit hysteresis due to the formation of inter-chain interactions that prevent the recovery of a collapsed chain conformation for extended time periods. Such a hysteretic response can be useful for mediating the sensitivity of responsive behavior or dampening the effect fluctuations. For instance, pH-controlled valves have been fabricated from track-etched membranes by modifying the pores with poly(allylamine hydrochloride) (PAH)/poly(sodium 4-styrenesulfonate) (PSS) layer-by-layer multilayers.⁶⁶ In this system, pH-dependent ionization and hydrophobic association of free amine groups of PAH follow a discontinuous trend,^{54,64} leading to hysteretic swelling of the multilayer. This mechanism practically enabled stable open or closed pores obtained at a single pH.

Inter-chain interactions can lead to long-term hysteretic responsive behavior, or even irreversible surface rearrangements, in membrane systems. An example of this is observed in membranes featuring pores lined with densely packed poly(acrylic acid) (PAA) brushes, designed for pH-responsive behavior.⁶⁹ When exposed to high pH, the PAA chains deprotonate and adopt extended configurations due to electrostatic repulsions between anionic carboxylate groups on the backbone. When the pH is reduced again, the carboxylate groups get protonated and form inter-chain hydrogen bonds between these extended chains, creating a physically cross-linked network. As a result, the chains do not collapse as expected. Even when the pH goes back to a higher value, these hydrogen bonds remain stable. This hysteretic and long-term rearrangement is highly dependent on the polymer architecture and conformation. For instance, very short chains or loops are unlikely to exhibit such rearrangement due to the difficulty of forming inter-chain bonds even in a swollen state. This type of

hysteresis is also more likely to occur in a dense brush than in a brush of spaced out chains. An irreversible surface rearrangement can be useful for tuning or improving the surface chemistry and/or morphology of a material simply by immersing it into a solution to induce polymer chain rearrangement. It can also serve as a sensor that is triggered with only brief exposure to the analyte.

Due to the high degrees of self-association possible between zwitterionic groups, a similar hysteretic or irreversible rearrangement may be possible upon exposure to solutions with high ionic strength. This would require a dense enough brush of polyzwitterion chains covering the membrane surface and pores, such as those created when a comb copolymer is used as an additive. If the chains cover the membrane surface and pore walls, this type of surface rearrangement would not only change the surface morphology and hydrophilicity, but also the permeation properties of the membrane. In addition, the presence of a polymer brush covering a membrane surface may also enhance fouling resistance by creating a steric barrier that prevents the access of foulants to the membrane surface.^{41,46} While the comb architecture has been studied for creating fouling-resistant poly(ethylene oxide) (PEO) brushes on membrane surfaces by blending,^{41,42,47,72} it is fairly unexplored in creating zwitterionic membranes. While a couple of studies exist that use zwitterionic comb copolymers to prepare membranes,^{52,73} the effect of copolymer architecture on surface segregation, membrane morphology, membrane performance or ionic strength has not been previously explored, especially in comparative studies that include more than one type of polymer architecture. In this paper, we compare the effect of random and comb-shaped zwitterionic copolymer additives used in the manufacture of PVDF-based ultrafiltration (UF) membranes on membrane performance. We demonstrate that comb-shaped copolymer additives exhibit irreversible conformational rearrangement upon exposure to saline solutions that result in smaller pore size and enhanced fouling resistance, while random copolymer additives exhibit small, mostly reversible changes in performance with feed ionic strength. As the random copolymer, we used poly(methyl methacrylate-*random*-sulfobetaine-2-vinyl pyridine) (PMMA-*r*-SB2VP) synthesized by free radical polymerization, based on the superior protein and oil fouling resistance of membranes prepared with it in our previous study.⁴⁰ A comb-shaped copolymer with a PVDF backbone and SB2VP side-chains, prepared by controlled radical polymerization with a similar SB2VP content, was used as a comparison. Membranes were prepared from blends of PVDF containing up to 5 wt% of each zwitterionic copolymer. Both copolymers led to membranes with similar initial water permeance. However, membranes prepared using the comb copolymer showed a remarkably more pronounced and irreversible decline in permeance with increasing ionic strength, as well as significant changes in the surface morphology and chemistry as documented by atomic force microscopy (AFM) and X-ray photoelectron spectroscopy (XPS). In contrast, the random copolymer additive led to smaller, mostly reversible changes in flux. In addition, the comb copolymer containing membrane showed stronger resistance to dynamic fouling by

a saline oil-in-water emulsion and to simulated protein adsorption in AFM force measurements. These results indicate that the polyzwitterion side-chains in the copolymer additive are able to segregate to the membrane surface and exhibit stable rearrangement upon exposure to saline water, leading to permanent changes in permeance, surface morphology and fouling resistance. The resultant membranes are more resistant to fouling than their counterparts prepared with random copolymer additives. This both introduces a novel approach for creating highly fouling resistant membranes and provides insights into how the configuration of zwitterionic groups on a membrane surface can influence the ionic strength response.

2. Experimental

2.1. Materials

Methyl methacrylate (MMA), 2-vinylpyridine, 1,3-propanesultone, azobisisobutyronitrile (AIBN), monomethyl ether of hydroquinone (MEHQ), *N,N,N',N'',N'''*-pentamethyldiethylenetriamine (PMDETA), copper(II) chloride (CuCl₂), L-ascorbic acid, bovine serum albumin (BSA, 66.5 kDa), ovalbumin from chicken egg white (42.7 kDa), β -lactoglobulin (18.4 kDa) from bovine milk, vitamin B12 (1.4 kDa), phosphate buffered saline (PBS) packs (0.138 M sodium chloride, 0.0027 M potassium chloride, pH 7.4), sodium chloride (NaCl) and lithium chloride (LiCl) were all purchased from Sigma Aldrich (St. Louis, MO). Cytochrome C (12.4 kDa), equine heart, +90%, was purchased from Alfa Aesar (Ward Hill, MA). Poly(vinylidene fluoride-*co*-chlorotrifluoroethylene) (PVDF-*co*-CTFE, M_n 149 kDa) was acquired from Solvay Specialty Polymers (Princeton, NJ). Basic activated alumina, dimethyl sulfoxide (DMSO), toluene, ethanol, hexane, trifluoroethanol (TFE), and methanol were all obtained from VWR (West Chester, PA). Deuterated dimethyl sulfoxide (DMSO-*d*₆) was purchased from Cambridge Isotope Laboratory (Tewksbury, MA). The DC193 surfactant was purchased from Dow Chemicals (Providence, RI). All chemicals and solvents were of reagent grade and used as received, except MMA, which was passed through a basic activated alumina column to eliminate any inhibitor present in it. The base material for our blend membranes was a copolymer of polyvinylidene fluoride (PVDF, KYNAR® grade 761) for membrane applications, provided by Arkema Inc. (King of Prussia, PA) in powder form.

2.2. Synthesis and characterization of zwitterionic amphiphilic copolymers

2.2.1. Synthesis of the PMMA-*r*-SB2VP copolymer. The random copolymer poly(methyl methacrylate-*random*-sulfobetaine-2-vinyl pyridine) (PMMA-*r*-SB2VP) was prepared following a free radical polymerization procedure elaborated in our previous study (Fig. 1A).⁴⁰ Briefly, 23.4 g (25.2 mL) MMA and 6.6 g SB2VP were dissolved in 110 mL TFE in a 250 mL round bottom flask at room temperature. 0.03 g of the initiator AIBN was added after dissolution. The reaction mixture was purged with nitrogen for 30 min. The reaction was conducted by stirring at 320 rpm for 48 hours at 60 °C. It was terminated by air

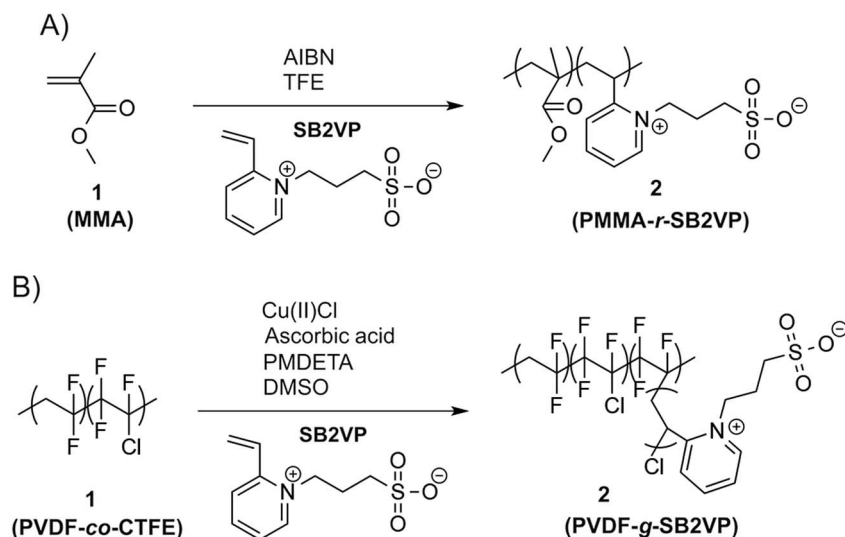


Fig. 1 Synthesis scheme for (A) free radical polymerization (FRP) of the random copolymer PMMA-*r*-SB2VP, and (B) activators regenerated by electron transfer atom transfer radical polymerization (ARGET-ATRP) of the comb copolymer PVDF-*g*-SB2VP.

exposure and the addition of 1.5 g MEHQ. Then, the reaction mixture was poured into a 1 : 1 mixture of hexane and ethanol to precipitate out the copolymer, followed by three methanol washes for eliminating any remaining unreacted monomer. The solid polymer attained was dried for two days under a fume hood and two more days in a vacuum oven at 50 °C. The product yield was found to be 75%, calculated from the ratio of the mass of the product copolymer to the mass of the monomers used. The chemical composition of the copolymer was determined by ^1H NMR (Bruker Avance III 500 MHz spectrometer, DMSO- d_6).

2.2.2. Synthesis of the PVDF-*g*-SB2VP copolymer. To synthesize the comb copolymer poly(vinylidene fluoride-*graft*-sulfobetaine-2-vinyl pyridine) (PVDF-*g*-SB2VP), we used the commercially available PVDF-based copolymer poly(vinylidene fluoride-*co*-chlorotrifluoroethylene) (PVDF-*co*-CTFE), which includes chlorine (Cl) atoms, as a macroinitiator forming the backbone of the copolymer. The molar ratio between PVDF and chlorotrifluoroethylene (CTFE) was reported in a previous study as $\sim 11 : 1$ (14 wt% CTFE), obtained by ^{19}F NMR.⁷⁴ The polymerization of the zwitterionic SB2VP monomer was initiated from Cl atoms of CTFE repeat units using activators regenerated by electron transfer atom transfer radical polymerization (ARGET-ATRP) (Fig. 1B). First, 2 g PVDF-*co*-CTFE and 9.8 g SB2VP were dissolved in 350 mL DMSO in a 1 L round bottom flask at 67 °C to make a ~ 3 wt% solution. After complete dissolution, the mixture was purged with nitrogen for at least 1 hour. In another 1 L round bottom flask, 0.65 g copper(II) chloride (CuCl_2), 3 mL N,N,N',N',N'' -pentamethyldiethylenetriamine (PMDETA) and 2 g ascorbic acid (AsAc) were added. The solution containing PVDF-*co*-CTFE and the monomer was quickly poured into this flask. The flask was sealed and placed in a pre-heated oil bath set at 70 °C with stirring at 400 rpm. The headspace was purged with nitrogen for 10 minutes, and the reaction was allowed to run for 24 hours. Polymerization was stopped by cooling, exposure to air, and the addition of 0.6

g MEHQ. The reaction mixture was precipitated into a 1 : 1 mixture of hexane and ethanol, and collected by filtration. The solid polymer was first washed overnight with ethanol, and then washed twice overnight with deionized water. For drying, the polymer was kept for two days under a fume hood and two more days in a vacuum oven at 50 °C. The copolymer composition and side-chain length were determined using peak ratios from ^1H NMR (Bruker Avance III 500 MHz spectrometer, DMSO- d_6) spectra and the PVDF : CTFE molar ratio of $\sim 11 : 1$ for the backbone, calculated from ^{19}F NMR. The percentage of initiated Cl was determined by comparing the ^{19}F NMR spectra of the backbone PVDF-*co*-CTFE and the product PVDF-*g*-SB2VP.

2.2.3. Molecular weight characterization. To estimate the molecular weight of the random copolymer PMMA-*r*-SB2VP, dynamic light scattering (DLS) measurements were performed with a Nano Brook 90Plus PALS particle sizer (Brookhaven Instruments, Holtsville, NY). The light source of the instrument was a He-Ne laser with a nominal wavelength of 659 nm and 1 mm entrance aperture. The measurements were conducted on a 1 mg mL^{-1} copolymer solution in dimethyl sulfoxide (DMSO) at a scattering angle of 90° and temperature 25 °C. Prior to any measurement, the copolymer solution was passed through a 0.2 μm glass fiber syringe filter to eliminate impurities. Five consecutive runs were performed after a stabilization period of two minutes. The effective hydrodynamic radius was used to attain the relative molecular weight based on PAN standards in dimethyl formamide (DMF) by implementing the Mark-Houwink equation. The Mark-Houwink parameters used for PAN in DMF at 25 °C were $K = 2.43 \times 10^{-2}$ and $a = 0.75$.⁷⁵

The molecular weight of the comb copolymer PVDF-*g*-SB2VP was estimated using the backbone PVDF-*co*-CTFE molecular weight (Solvay Specialty Polymers, M_n 149 kDa) and the backbone : side-chain weight ratio obtained by ^1H NMR.

2.3. Membrane preparation with zwitterionic copolymer additives

Ultrafiltration (UF) membranes were cast from blends of a grade of PVDF manufactured by Arkema Inc. for membrane applications with the synthesized zwitterionic copolymers (either random PMMA-*r*-SB2VP or comb-shaped PVDF-*g*-SB2VP) by non-solvent induced phase separation (NIPS). Dimethyl sulfoxide (DMSO) was used as the solvent because it could dissolve PVDF and both of the zwitterionic copolymers at relevant concentrations. The ratios between the random or comb copolymer additive : PVDF were fixed at 2 : 98 and 5 : 95 by weight, totaling 3 g of polymer dissolved in 17 g (15.45 mL) DMSO. To prepare the membrane casting solutions, first the additive copolymer was completely dissolved in DMSO by stirring the solution at approximately 70 °C. After full dissolution, PVDF was added into the casting solution at 70 °C and then stirred overnight. The casting solutions in heat resistant glass vials were capped and degassed in a vacuum oven set at 50 °C for 24 hours. Each membrane was prepared by casting a film of the solution on a glass plate using an adjustable doctor blade (GardCo) set to a 150 micrometer gate height. The glass plate with the cast film was immersed in a water bath for 20 minutes to precipitate out the polymer and obtain the porous membrane, which was then moved to a fresh water bath. As a control, a PVDF membrane without any additive was formed by dissolving 3 g PVDF in 17 g (15.45 mL) DMSO and following the NIPS procedure mentioned above. All membranes were stored in a deionized water bath with the antibacterial preservative sodium metabisulfite.

2.4. Membrane morphology and surface hydrophilicity

The cross-sectional morphology of each membrane was visualized by using a scanning electron microscope (SEM, Phenom G2 Pure Tabletop SEM) operated at 5 kV. The cross section of each membrane sample was obtained by first immersing the membrane in liquid nitrogen and then breaking it into two pieces using tweezers. Prior to imaging, the freeze-fractured membranes were mounted on cross-sectional SEM stubs with double-sided carbon conductive tape and sputter coated with a gold–palladium (60–40) alloy for 120 s at 30 mA current in an argon atmosphere using a Cressington Sputter Coater 108 (Cressington Scientific Instruments, Watford, UK). SEM images were all acquired at a magnification of 1500×.

Membrane surface hydrophilicity was evaluated by contact angle measurements conducted using the captive air bubble method. The membranes were attached to a glass slide with double-sided tape while wet and immersed in deionized water upside down. A 2 µL air bubble was released from the tip of a U-shaped needle and placed on the surface of the membrane, still immersed in water. A Ramé-Hart contact angle instrument (Succasunna, NJ) equipped with a horizontal microscope and camera connected to a video screen was used for imaging. DROP image Advanced version 2.4.05 software was used for the analysis. For each data point, the external angle on the right side of the air bubble was measured at three different spots per

membrane and the mean value ±SD of three different samples was reported.

2.5. Measurement of water permeance and pore size

To measure the pure water permeance, filtration experiments were conducted using an Amicon 8010 stirred, dead-end filtration cell (Millipore) with a cell volume of 10 mL and an effective filtration area of 4.1 cm², connected to a 3.5 L dispensing tank. The membrane was first compacted by filtering deionized water for 2 hours at 10 psi (0.07 MPa) pressure. Following compaction, the permeance was measured at 10 psi (0.07 MPa) using a cell stirred at 500 rpm. A Scout Pro SP401 balance connected to a Dell laptop was used to automatically record the permeate weight every 30 seconds with TWedge 2.4 software (TEC-IT, Austria). The membrane permeance was obtained by normalizing the flux with applied pressure and expressed as

$$L_p = \frac{J}{\Delta P}$$

where L_p is the membrane permeance (L m⁻² h⁻¹ bar⁻¹), J is the flux (L m⁻² h⁻¹), which is the water flow rate normalized by the active membrane area, and ΔP is the applied pressure (bar).

To characterize the pore size of the membranes, we filtered a series of solutes with varying molecular weights and hydrodynamic radii (R_H) at 10 psi (0.07 MPa), and measured their rejection. These solutes included four proteins : bovine serum albumin (BSA, 66.5 kDa, R_H ~3.5 nm), ovalbumin (42.7 kDa, R_H ~2.8 nm), β-lactoglobulin (18.4 kDa, R_H ~2 nm), and cytochrome C (12.4 kDa, R_H ~1.7 nm). For a smaller solute, we also filtered vitamin B12 (1.4 kDa, R_H ~0.65 nm). Each solute was dissolved at a concentration of 1 g L⁻¹ in 0.01 M PBS solution (pH 7.4) and filtered one at a time through the membranes. The first 1–2 mL of filtrate was discarded. Solute concentration in the subsequent 2 mL of filtrate was measured and used to calculate rejection, which is expressed as

$$R\% = \left(1 - \frac{C_P}{C_F}\right) \times 100$$

where R is the solute rejection (%), C_F is the feed concentration (1 g L⁻¹), and C_P is the permeate concentration (g L⁻¹). Solute concentration in the feed and permeate was quantified by UV-vis spectroscopy (Thermo Scientific Genesys 10S spectrometer, Waltham, MA) at 280 nm for BSA, ovalbumin, and β-Lactoglobulin, at 410 nm for cytochrome C, and at 360 nm for vitamin B12. For each data point, three swatches from the same membrane sheet were tested.

2.6. Characterizing changes in membrane properties due to ionic strength

To characterize changes in the membrane surface morphology and chemistry upon exposure to high ionic strength solutions, membrane samples were prepared with two procedures: (1) air drying a swatch from the membrane stored in water, or (2) cutting out a swatch from the membrane stored in water, immersing it overnight in 0.1 M NaCl, immersing it back in deionized water for one hour, and then air drying. Before air

drying, each membrane was dipped in liquid nitrogen to limit surface rearrangement.

The near surface composition of the zwitterionic additive containing membranes prepared using these two methods were determined by X-ray photoelectron spectroscopy (XPS) analysis. The experiments were conducted on rectangular pieces of 1 cm \times 1 cm using a K-alpha X-ray photoelectron spectrometer (Thermo Scientific, Waltham, MA) equipped with a monochromatic Al K α source (1486.6 eV) and an electron takeoff angle of 90° relative to the sample plane. A survey scan and a high resolution scan of the C 1s peak were run for each sample.

To determine changes in the surface nanostructure upon exposure to saline water, the membrane samples described above were analyzed employing atomic force microscopy (AFM) measurements with a Dimension 3100 AFM (Veeco, Plainview, NY) in tapping mode. For the measurements, the membrane samples were mounted on a glass slide with double-sided tape after drying. AFM cantilevers were obtained from Bruker with an 8 nm nominal tip radius, $f_0 = 50$ –100 kHz and $k = 1$ –5 N m $^{-1}$. AFM micrographs from 10 \times 10 μm^2 surface sections were obtained in tapping mode, and the surface roughness of each membrane was measured using Gwyddion software.

The change in membrane permeance with ionic strength was studied by dead-end filtration of NaCl solutions with different concentrations (0–1 M) at 10 psi (0.07 MPa). The permeance of each NaCl solution was calculated by normalizing the average flux by filtration pressure.

2.7. Oil/water emulsion fouling experiments

Before oil fouling tests, membranes were compacted by filtering deionized water for at least 2 hours at 10 psi (0.07 MPa). Data shown in the plots were collected after this compaction period. Oily water filtration experiments were performed employing the set up described above for water permeance measurements. Model oil-in-water emulsions contained 1.5 g L $^{-1}$ soybean oil mixed with the non-ionic surfactant DC193 (9 : 1 ratio of soybean oil : DC193 surfactant) in either 0.1 M NaCl or deionized water. To attain a stable oil-in-water emulsion, the foulant mixture was vigorously mixed using a blender for 3 minutes. The first oil fouling cycle was run in 0.1 M NaCl solution with the following steps: (1) filtering 0.1 M NaCl solution for 2 hours to measure the initial flux, (2) filtering oil-in-water emulsion in 0.1 M NaCl solution for 24 hours to simulate fouling, and (3) after washing the cell and the membrane several times with 0.1 M NaCl, filtering 0.1 M NaCl solution again for 2 hours to compare the flux before and after oil-in-water emulsion filtration. Subsequent to this, we performed another oil fouling cycle that involved the same three steps, but in deionized water instead of 0.1 M NaCl solution.

2.8. Protein fouling experiments

Protein fouling experiments were conducted using the same set-up as above using 1 g L $^{-1}$ BSA solution in PBS at pH 7.4. In these tests, we followed the following steps: (1) filtering PBS for 2 hours to condition the membrane, (2) filtering deionized water

for 2 hours to determine the conditioned initial flux, (3) filtering BSA solution in PBS for 24 hours to simulate protein fouling, and (4) after rinsing the membrane and cell several times with PBS, filtering deionized water for 2 hours again to compare fluxes before and after fouling.

2.9. Organic fouling propensity from AFM jump-to-force measurements

A Bruker Multimode 8 atomic force microscope equipped with a Nanoscope V, Pico Force controller, and fluid cell (Bruker AXS, Santa Barbara, CA) was used to measure the jump-to-force measurements between foulant and membrane surfaces. As the model organic foulant, we employed a 11.6 μm carboxylate modified latex particle (ThermoFisher Sci., Pittsburgh, PA) attached to a triangular cantilever (Bruker Nano Inc., Camarillo, CA) with a nominal spring constant of 0.1 N m $^{-1}$. AFM was operated in force mode. The approach curve was terminated once a force of 1 nN was applied and retraction was initiated, at a rate of 1 μm s $^{-1}$. The experiments were conducted at room temperature in a liquid cell containing PBS solution at pH 7.4. For each membrane, 8 to 10 spots were sampled, where each spot was split into a 5 by 5 grid covering a square of 2 μm \times 2 μm , acquiring 25 force curves per spot.

3. Results and discussion

3.1. Synthesis and characterization of zwitterionic copolymers

Most approaches to manufacturing membranes with improved fouling resistance involve modification of existing membranes with hydrophilic groups, with methods such as plasma treatment,⁷⁶ grafting of hydrophilic polymers,^{51,53,77–81} or the application of a hydrophilic coating.^{29–31,82–85} However, it is possible to form membranes with hydrophilic, fouling-resistant surfaces without added manufacturing steps by blending an amphiphilic copolymer additive with the commodity polymer more commonly used for membrane manufacture, and preparing the membrane using standard techniques such as NIPS. The hydrophilic segments drive the copolymer to the polymer/water interface, creating a more fouling-resistant membrane surface and improving wettability. While several groups have used this general approach, the thoughtful design of the amphiphilic copolymer is crucial for achieving high degrees of fouling resistance without sacrificing selectivity and other properties. For instance, in most cases, amphiphilic copolymer additives containing higher fractions of the hydrophilic monomer lead to increased fouling resistance.^{41,42,72} However, when zwitterionic random copolymers are used as additives, high zwitterionic repeat unit content can lead to poor compatibility during the membrane formation process, resulting in poor performance.⁴⁰ In particular, the copolymer architecture can have a distinct influence on both surface segregation and foulant–membrane interactions.^{42,44,45,72}

In this study, our goal was to compare the performance of two zwitterion-containing copolymers of similar chemical structures, yet different polymer architecture, as additives to

PVDF during the formation of membranes by NIPS. These copolymers need to contain hydrophobic segments compatible with the commodity base polymer, PVDF, to anchor the zwitterionic units to the membrane.^{46,72} The hydrophilic segments (short sequences of zwitterionic repeat units in a random copolymer, or short zwitterionic side-chains in the comb copolymer) segregate to the membrane surface, which is exposed to water, to minimize the surface energy of the system. Our goal was to explore how the different copolymer architectures lead to differences in surface segregation. Furthermore, the resultant membranes will have different arrangements of zwitterionic groups on their surfaces. It is expected that the surface of membranes prepared from the random copolymers will have either single zwitterionic groups or very short zwitterionic segments constrained on both ends. In contrast, the comb copolymer is expected to create a polyzwitterion brush on the top surface and in membrane pores. These differences will likely lead to variations in fouling resistance and ionic strength response.

As the random copolymer, we chose to use a statistical copolymer of methyl methacrylate (MMA) and the zwitterionic monomer SB2VP. We have shown that this copolymer can be used as an additive to PVDF to create highly fouling-resistant membranes, but only if the copolymer contained a relatively low mass fraction of the zwitterionic monomer.⁴⁰ We synthesized this copolymer following the same procedure, using free radical polymerization (Fig. 1A).⁴⁰ The synthesized copolymer, PMMA-*r*-SB2VP, was found to contain 25 wt% SB2VP using ¹H NMR spectroscopy in DMSO-*d*₆ (Fig. S1, ESI†). The molecular weight was estimated by dynamic light scattering (DLS) measurements in DMSO. The hydrodynamic radius of the copolymer was found to be 55 ± 4 nm. Using the Mark-Houwink equation based on PAN standards in DMF,⁷³ the relative molecular weight of the copolymer was calculated to be 360 kDa. While this value is an absolute molar mass, it indicates that long copolymer chains were formed, significantly above the entanglement molecular weight (~10 kDa for PMMA).⁸⁶

To serve as the comb copolymer additive, we initially prepared a comb copolymer with a PMMA backbone and SB2VP side-chains, targeting a similar SB2VP mass fraction. Interestingly, this copolymer was highly water soluble, even when prepared with quite short side-chains and zwitterion contents as low as 10–15 wt%. This meant that these PMMA-*g*-SB2VP copolymers could not be used as membrane additives, at least in a way comparable to the behavior of the water-insoluble random copolymer. This comb copolymer would dissolve away during membrane preparation. Some of it may be stuck on the membrane surface through entanglements, but leach slowly during use.

Therefore, we decided to use an alternative backbone that is still miscible with PVDF to prepare this comb copolymer additive. We designed a synthesis scheme that would result in a PVDF backbone and SB2VP side-chains. To synthesize this comb copolymer, PVDF-*g*-SB2VP, a commercially available PVDF-based copolymer that contains chlorotrifluoroethylene (CTFE) repeat units, PVDF-*co*-CTFE, was used as a macro-initiator in activators regenerated by Electron Transfer Atom Transfer Radical Polymerization (ARGET-ATRP). The molar

ratio between PVDF and CTFE was determined to be ~11 : 1 (14 wt% CTFE) in a previous study using ¹⁹F NMR.⁷⁴ The zwitterionic SB2VP side-chains were grown from initiating chlorine atoms on CTFE repeat units using ARGET-ATRP (Fig. 1B), which is a living polymerization method that is initiated at Cl atoms and catalyzed by copper complexes.

The ¹H-NMR spectrum of the synthesized PVDF-*g*-SB2VP, showing peak assignments, is presented in Fig. 2. Each SB2VP unit was associated with four protons appearing in the 7.5–9.5 ppm region (d, e, f and g). The broad peaks around 4.1 and 4.8 ppm were attributed to the CH (c) protons and CH₂ (h) protons from SB2VP. The peak at 2.2 ppm was assigned to the convolution of CH₂ protons from SB2VP (b) and head-to-head CH₂ protons from PVDF (a hh), whereas the peak at 2.9 ppm was assigned to the head-to-tail CH₂ protons from PVDF (a ht). The ratio of these peaks, together with the PVDF : CTFE molar ratio (PVDF : CTFE molar ratio ~11 : 1) obtained from the backbone PVDF-*co*-CTFE ¹⁹F NMR, was employed to calculate the comb copolymer composition. We determined that 85% of Cl atoms initiated the polymerization of SB2VP by comparing the ¹⁹F NMR spectra of the backbone PVDF-*co*-CTFE and the product PVDF-*g*-SB2VP (Fig. S2, ESI†). The PVDF-*g*-SB2VP copolymer synthesized was extracted with water to eliminate water soluble polymer fractions. The ¹H-NMR spectrum after water wash (Fig. S3, ESI†) showed the final copolymer to comprise ~26 wt% SB2VP, corresponding to 1–2 SB2VP repeat units on average at each initiating Cl site. The water-soluble fractions of the copolymer could have longer average side-chain lengths. It is also possible (and even likely) that this average side-chain length is polydisperse, with sparse but longer side-chains. The SB2VP weight percentage in the random and comb copolymers is comparable, as intended. The molecular weight of PVDF-*g*-SB2VP was estimated to be ~200 kDa by calculating it from the backbone PVDF-*co*-CTFE molecular weight (Solvay Specialty Polymers, *M*_n 149 kDa) and the backbone : side-chain weight ratio.

3.2. Preparation and morphology of the blend membranes with zwitterionic additives

To observe the impact of copolymer additive architecture on the PVDF membrane performance and structure, we cast UF

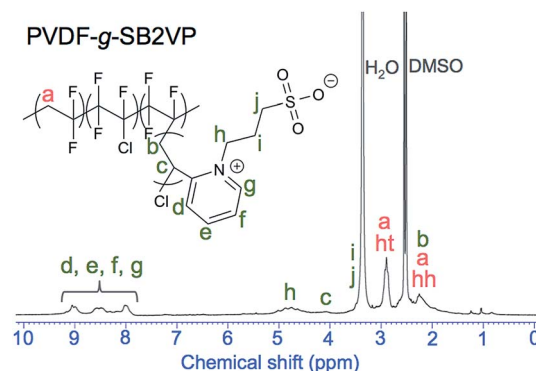


Fig. 2 ¹H-NMR spectrum of the zwitterionic comb copolymer PVDF-*g*-SB2VP.

Table 1 Blend and control PVDF membranes prepared in this study

Membrane series	Membrane code	Additive	Additive : PVDF ratio
Additive-free PVDF	M-PVDF	None	0 : 100
	M-R	PMMA- <i>r</i> -SB2VP	2 : 98
	M-R5		5 : 95
M-C	M-C2	PVDF- <i>g</i> -SB2VP	2 : 98
	M-C5		5 : 95

membranes by blending a 2 or 5 wt% zwitterionic additive in the PVDF base during NIPS. We could not incorporate the comb copolymer at higher ratios because of its solubility limit in DMSO. An additive free PVDF membrane was also cast as a control. All membranes used in this study are presented in Table 1.

The membrane morphology was examined by imaging freeze-fractured cross-sections of the membranes by SEM (Fig. 3). The membranes are highly porous, displaying a typical asymmetric UF morphology with large macrovoids in each case. There is no observed macrophase separation of the zwitterionic additive from the base PVDF, which could lead to a substantial decline in the membrane performance.⁴⁰ Tilted cross-sectional SEM images showing both the surface and cross-sectional morphologies of the membranes are given in Fig. S4, ESI.†

3.3. Surface hydrophilicity, water permeance, and pore size

Surface segregation of the zwitterionic copolymers is expected to improve the surface hydrophilicity of membranes prepared from their blends. As zwitterionic random copolymers can undergo fast surface rearrangement upon drying,⁸⁷ we

documented surface hydrophilicity using captive air bubble contact angle measurements. This method ensures that the membrane is fully wetted during characterization, closely simulating the operating environment during filtration. Indeed, captive bubble contact angle measurements (Fig. 4A) show a remarkable improvement in surface hydrophilicity with increasing content of either additive. Interestingly, the copolymer architecture had little effect on the resultant surface hydrophilicity. The average contact angle of 5 wt% additive containing membranes in both series (M-R5 and M-C5) was found to be $\sim 33^\circ \pm 3^\circ$, whereas the additive free M-PVDF had a contact angle of $55^\circ \pm 4^\circ$. This enhancement in hydrophilicity indicates the segregation of zwitterionic groups to the membrane surface, as desired.

It should be noted that the contact angle of the additive-free PVDF membrane is lower than the previously reported value of $93^\circ \pm 4^\circ$.⁴⁰ The previous study was conducted using PVDF sourced from Sigma Aldrich. In this study, we aimed to gain more industrially relevant insights and used a PVDF grade designed for use in membrane manufacturing, generously supplied by Arkema Inc. (King of Prussia, PA). While not clearly identified in the supplier's literature, we believe that this material is not a PVDF homopolymer, but instead a PVDF-based copolymer that is designed to be more hydrophilic. Importantly, this change did not lead to issues with poor miscibility or decreased surface segregation of the zwitterionic copolymers, demonstrating the applicability of the blending approach in a wider array of industrial contexts.

Fig. 4B shows the pure water permeance of the different membranes prepared in this study. The addition of 2 wt% of either the random or the comb copolymer (M-R2 and M-C2) did not lead to a significant increase in permeance compared with

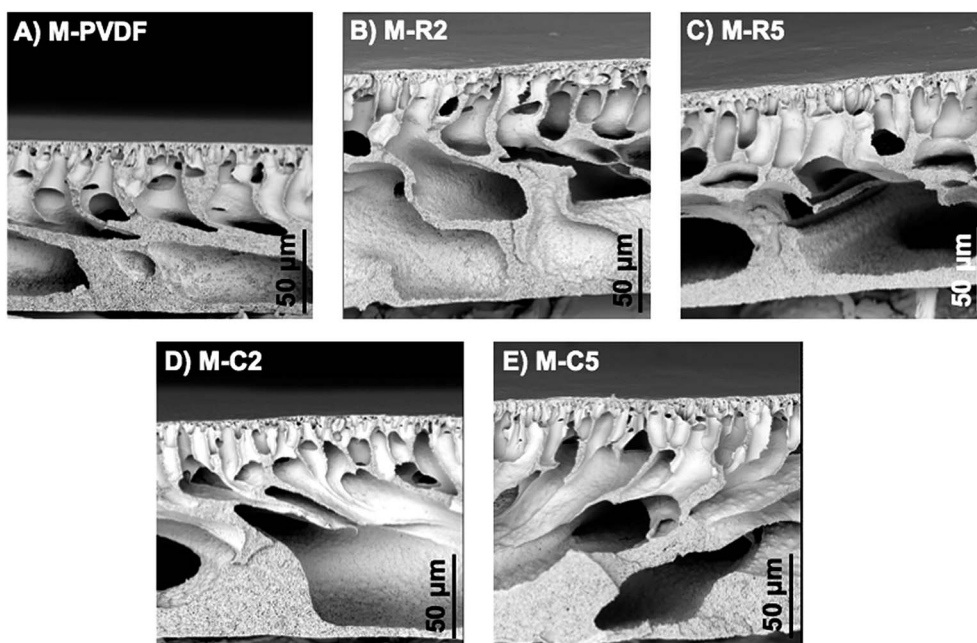


Fig. 3 Cross-sectional SEM images of membranes with random and comb additives. From left to right (A) M-PVDF, (B) M-R2, (C) M-R5, (D) M-C2, and (E) M-C5.

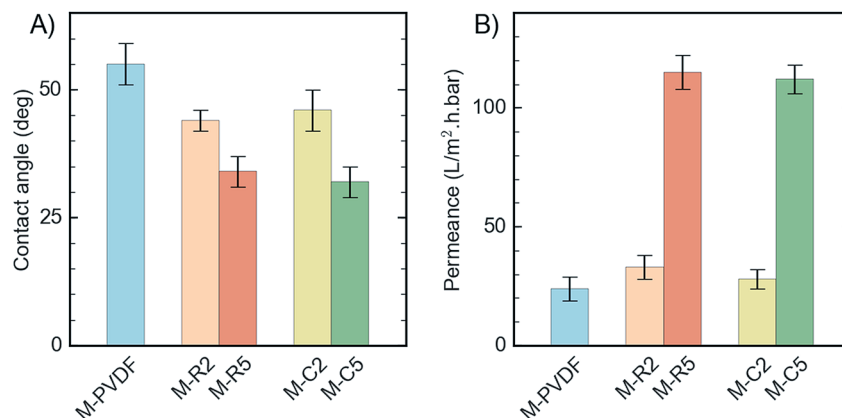


Fig. 4 (A) Contact angle and (B) pure water permeance of blend membranes prepared with zwitterionic random and comb copolymer additives, along with the control M-PVDF.

the M-PVDF membrane. This may be because the use of only 2 wt% copolymer additive did not lead to sufficient surface segregation and coverage to significantly improve permeance. The low concentration of the additive may also be insufficient to act as a good pore former. In contrast, when the additive content was increased to 5 wt%, the water permeance increased to over $110 \text{ L m}^{-2} \text{ h}^{-1} \text{ bar}^{-1}$, nearly five times that of M-PVDF ($24 \pm 5 \text{ L m}^{-2} \text{ h}^{-1} \text{ bar}^{-1}$). M-R5 and M-C5 membranes had comparable permeances, indicating that the copolymer architecture did not have a significant effect on the enhancement of pure water permeability. All contact angle and permeance values shown in Fig. 4 are also listed in Table S1, ESI†.

Based on these results, we further characterized the M-R5 and M-C5 membranes, which had comparable surface hydrophilicity and permeance values. To characterize their selectivity, we dissolved a series of molecules with varying sizes in 0.01 M PBS buffer (pH 7.4, ionic strength 0.14 M), filtered them through each membrane at 10 psi (0.07 MPa), and then measured their rejection. We screened the rejection of the small molecule vitamin B12 (1.4 kDa, $R_H \sim 0.65 \text{ nm}$) and four proteins including cytochrome C (12.4 kDa, $R_H \sim 1.7 \text{ nm}$), β -Lactoglobulin (18.4 kDa, $R_H \sim 2 \text{ nm}$), ovalbumin (42.7 kDa, $R_H \sim 2.8 \text{ nm}$)

and BSA (66.5 kDa, $R_H \sim 3.5 \text{ nm}$). Both M-R5 and M-C5 membranes exhibited similar rejection curves, demonstrating sharp selectivity with a molecular weight cut-off (MWCO) of around $\sim 18 \text{ kDa}$ (Fig. 5). This corresponds to a nominal pore size of $\sim 4 \text{ nm}$. The rejection of these proteins by the M-PVDF membrane was slightly higher (Table S2, ESI†), corresponding to a nominal MWCO of $\sim 15 \text{ kDa}$ and an estimated nominal pore size slightly below 4 nm . However, this slight decrease in effective pore size was not sufficient to justify the drastically lower permeance. Despite the high water permeances observed and large macrovoids in the support layer, the M-R5 and M-C5 membranes still show sharp selectivity, which leverages them as competitive candidates for UF applications.

3.4. Changes in the surface composition, nanostructure and water permeance upon exposure to high ionic strength solutions

The data up to this point show that additive copolymer architecture has little effect on the morphology, surface chemistry, and performance of the resultant membranes. These membranes had similar deionized water permeances and protein rejections. However, the increased mobility of zwitterionic groups in the membrane prepared from the comb-shaped copolymer, M-C5, may lead to differences in how they respond to changes in ionic strength. To test this phenomenon, we filtered NaCl solutions of increasing concentration through the M-R5 and M-C5 membranes and monitored their permeance (Fig. 6). The permeance of M-R5 exhibited a relatively minor change with ionic strength. The permeance declined by at most $\sim 20\%$ of its initial value when the NaCl concentration was increased to 0.15 M. When the feed was switched back to deionized water, the permeance recovered to 91% of its initial value, within the error margin. Even if the hydrophilicity of the zwitterionic groups increased, the short segment length and limited mobility of these groups would prevent them from expanding into the pores and occluding them. Any such changes in conformation would likely lead to minimal changes in the effective pore size of $\sim 4 \text{ nm}$, significantly larger than the

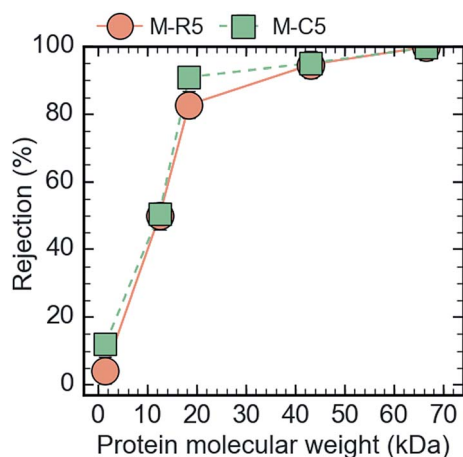


Fig. 5 Protein rejection of M-R5 and M-C5 membranes.

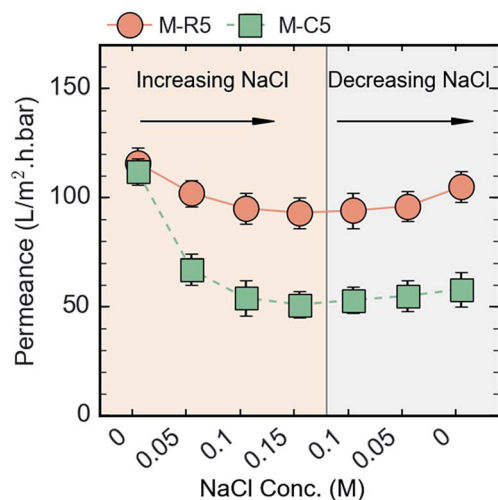


Fig. 6 Permeance of M-R5 and M-C5 membranes with increasing NaCl concentration.

measured distance between the SB2VP backbone and the farthest atom (see ESI, Section S5†).

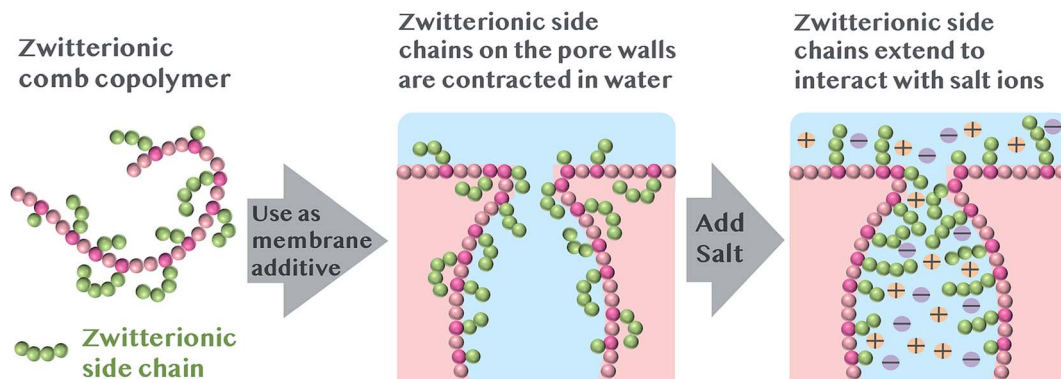
In contrast, M-C5 showed a sharp drop in its permeance with increasing ionic strength. The permeance fell by over 50% upon exposure to 0.15 M NaCl. The poly(SB2VP) side-chains of the comb-shaped copolymer are much larger in size and have more conformational flexibility. The distance between the first and the farthest atom carbon of a short poly(SB2VP) chain, a trimer, was calculated to be ~ 1.0 – 1.1 nm, much larger in comparison to the monomer. Furthermore, the large number of flexible bonds in this oligomer structure means that the effective size of polyelectrolytic side-chains exposed to the pore can change much more significantly upon changes in hydrophilicity. Thus, this larger change in flux is in agreement with the molecular structure of the comb copolymer additive. Interestingly, this decrease was almost completely irreversible. This can be described as a stable hysteretic response or as a surface rearrangement in response to this exposure. Stimuli-responsive polymers usually exhibit a reversible response to external stimuli.^{33,54–61} This means that the material recognizes and responds to its instant environmental conditions only, with no memory of previous conditions, and thus, no hysteretic response. In rare cases, polymers with a hysteretic response to environmental stimuli have been reported.^{63–69} For porous membranes, almost in all cases, the hysteretic response has been found to dissipate with time.^{65–68} There is only one report of hysteretic and long lasting pH response in a nanoporous membrane,⁶⁹ stemming from strong hydrogen bonding between the uniquely dense poly(acrylic acid) (PAA) brushes lining the pore walls. Enduring hysteretic swelling was also observed in a polyampholyte gel comprising both anionic and cationic constituents, similar to a dense zwitterion brush found in our membrane, again due to various competing interactions.⁶³ Thus, we believe that this mostly irreversible response is enabled by the combination of strong self-association interactions that occur between zwitterionic sulfobetaine groups^{88,89} and the high density of the polyelectrolyte brush that is formed by the surface segregation of the comb-shaped copolymer.^{42,90}

In responsive membranes, changing the pore diameter typically dictates the change in permeance.^{91,92} In our M-C5 membrane, the pore diameter is strongly affected by the degree of swelling of the poly(SB2VP) side-chains. In pure water, it is likely that SB2VP repeat units either form intramolecular associations leading to relatively hydrophobic SB2VP repeat units or intra-chain interactions between SB2VP repeat units along the same side chain.⁹³ This results in contracted side chains as illustrated in Scheme 1 and therefore essentially completely open pores.

In saline water, added salt ions break some of the intramolecular and intra-chain interactions by charge screening.⁹⁴ SB2VP side chains extend from the pore walls to better access the salt ions (Scheme 1). The pore opening becomes narrower, decreasing the flow rate. Despite our NMR results indicating an average side chain length of 1–2 SB2VP repeat units, we see a significant drop in permeance by switching the feed to 0.15 M NaCl solution. This indicates that the side chain expansion is significant. This implies that the side chains are highly poly-disperse. The comb-shaped copolymer likely bears some longer SB2VP side chains as well as single monomers attached to the backbone, but at a low frequency. In addition, given the small ~ 4 nm pore size of the M-C5 membrane, conformational rearrangements even in the short SB2VP segments may lead to a marked change in pore size. For instance, the end-to-end distance of a fully extended, all-*trans* dimer of SB2VP is 0.5 nm, which is still comparable to the pore diameter. The permeance drop does not reverse with decreasing salt concentration, exhibiting a hysteretic response to ionic strength.

The irreversible permeance drop implies that the expanded conformation of zwitterionic side chains acquired in the saline environment is likely retained afterwards. The expanded conformational arrangement enables closer proximity between neighboring SB2VP side chains. This allows the formation of inter-chain dipole–dipole interactions between SB2VP units on neighboring side-chains when the feed is switched back to deionized water. In addition, the SB2VP groups are better exposed to water molecules in expanded conformation, which augments hydrogen bonding with water molecules. The hydrogen bonds are energetically favorable, but they limit the chain mobility.⁶³ In this system, the hydrogen bonding can stabilize the chain configuration fairly easily due to short segments that are almost fully surrounded by water molecules, as opposed to longer Gaussian chains with entanglements.

Based on the results above, we expected that the surface composition of these membranes, particularly that of M-C5 which exhibits irreversible performance changes, changes irreversibly upon exposure to high ionic strength solutions. To test this hypothesis, we immersed the M-R5 and M-C5 membranes in 0.1 M NaCl overnight, and then rinsed them in deionized water. This removed all salt ions; only irreversible changes in the surface chemistry and morphology remained. These membranes are referred to as “M-R5 after NaCl” and “M-C5 after NaCl”. We then analyzed the near-surface composition of these membranes by X-ray photoelectron spectroscopy (XPS), along with membranes that were not exposed to saline solutions (referred to as “M-PVDF as prepared”, “M-R5 as prepared”,



Scheme 1 Schematic showing zwitterionic comb copolymer assembly on the membrane pore walls and the conformational rearrangement of zwitterionic side chains in response to addition of salt ions.

and “M-C5 as prepared”). XPS characterizes the chemical composition of the top 1–10 nm of the membranes. This allows us to determine polymer rearrangement at the surface and identify functional groups that preferentially segregate to the polymer/water interface.

Fig. 7 shows the high-resolution C 1s scans from XPS measurements. The peak centered at 284.5 eV was assigned to C–C, C=C, and C–H groups. The peaks centered around 286 eV and 288 eV were linked to C–O/N/S and C=O groups, respectively. CF₂ functional groups from PVDF units led to the highest binding energy peak, appearing around 291 eV.^{95,96}

Even though the PVDF grade supplied by Arkema was not marketed as a copolymer, the surface of the membrane cast purely from this material, M-PVDF, exhibited a large fraction of C=O and C–O/N/S groups. The ratio of the peak corresponding to C–C, C=C, and C–H groups to that from CF₂ groups was 0.83 for this membrane, compared with 1 expected for a PVDF homopolymer. Survey scans (Table 2) indicated that the membrane surface features around 6.6% oxygen atoms, and a small number of nitrogen atoms. This indicates that the PVDF polymer used includes some hydrophilic groups, possibly some acrylate esters, amides, amines and/or carboxylic acid groups.

This complicates the analysis of the surface segregation of the zwitterionic copolymers, which contain many of the same atoms and functional groups. While nitrogen and sulfur atoms are present in the zwitterionic groups, they represent only one out of 15 measurable atoms in the SB2VP repeat unit. This atomic percentage is further diluted to barely above the instrument's detection limit by the presence of PMMA or PVDF groups in the copolymer and upon blending. In contrast, SB2VP repeat units are quite rich in carbon (10 out of 15 atoms) compared with PVDF. They also contain a larger fraction of C–C, C=C, and C–H groups, and no CF₂ groups. Therefore, to characterize the surface segregation of zwitterionic SB2VP groups, we chose to determine the ratio of C : F atoms obtained from survey scans, and the ratio of the peak corresponding to C–C, C=C and C–H groups to that for CF₂ groups obtained from high resolution C 1s scans.

When the random copolymer was blended with this PVDF (M-R5), the (C–C, C=C, C–H) : C–F₂ peak ratio increased from

0.83 to 4.3. This indicates that the surface concentration of PVDF, the only source of CF₂ groups, decreases. Instead, more C–C and C=C groups are exposed, likely from the SB2VP units on the copolymer. When the M-R5 membrane was immersed in saline solution, this (C–C, C=C, C–H) : CF₂ peak ratio further increased to 7.6, indicative of further enrichment of carbon-rich zwitterionic groups on the membrane surface and a decrease in the concentration of fluorinated groups from PVDF chains. This trend was corroborated by the surface elemental compositions acquired from XPS survey scans. The atomic ratio of C/F increased from 1.4 to 3 after random copolymer addition in PVDF, which then further increased to 5.2 after immersion of M-R5 in saline solution, representing enhanced zwitterionic group segregation near the surface.

The analysis of the membranes prepared from blends of this commercial PVDF with the comb copolymer was further complicated by the presence of CF₂ groups in the copolymer itself. The surface of the membrane appears somewhat similar to that of M-PVDF in atomic composition, though it exhibits fewer C=C, C–C, and C–H groups and more C–O/N/S groups according to the high resolution scans, which would be consistent with the presence of these groups on SB2VP. On the other hand, the compositional rearrangement of the surface could easily be tracked by comparing the high resolution C 1s scans of M-C5 membranes before and after immersion in 0.1 M NaCl. The (C–C, C=C, C–H) : CF₂ peak ratio jumped from 0.45 to 3.8 upon immersion in saline solution, which indicates a more drastic irreversible surface rearrangement in the near-surface composition compared with the random-additive-containing M-R5 membrane. To summarize, electrostatic interactions between the zwitterionic groups and salt ions in feed solution stimulate the rearrangement of zwitterionic groups on the membrane near surface in both additives. This effect is more prominent in membranes prepared with the comb copolymer additive, potentially due to the spatial mobility of the zwitterionic groups allowing easier reorganization. These results are in agreement with the observations from the filtration experiments.

In addition to changes in surface chemistry, we expected that exposure to a high ionic strength solution would also lead to

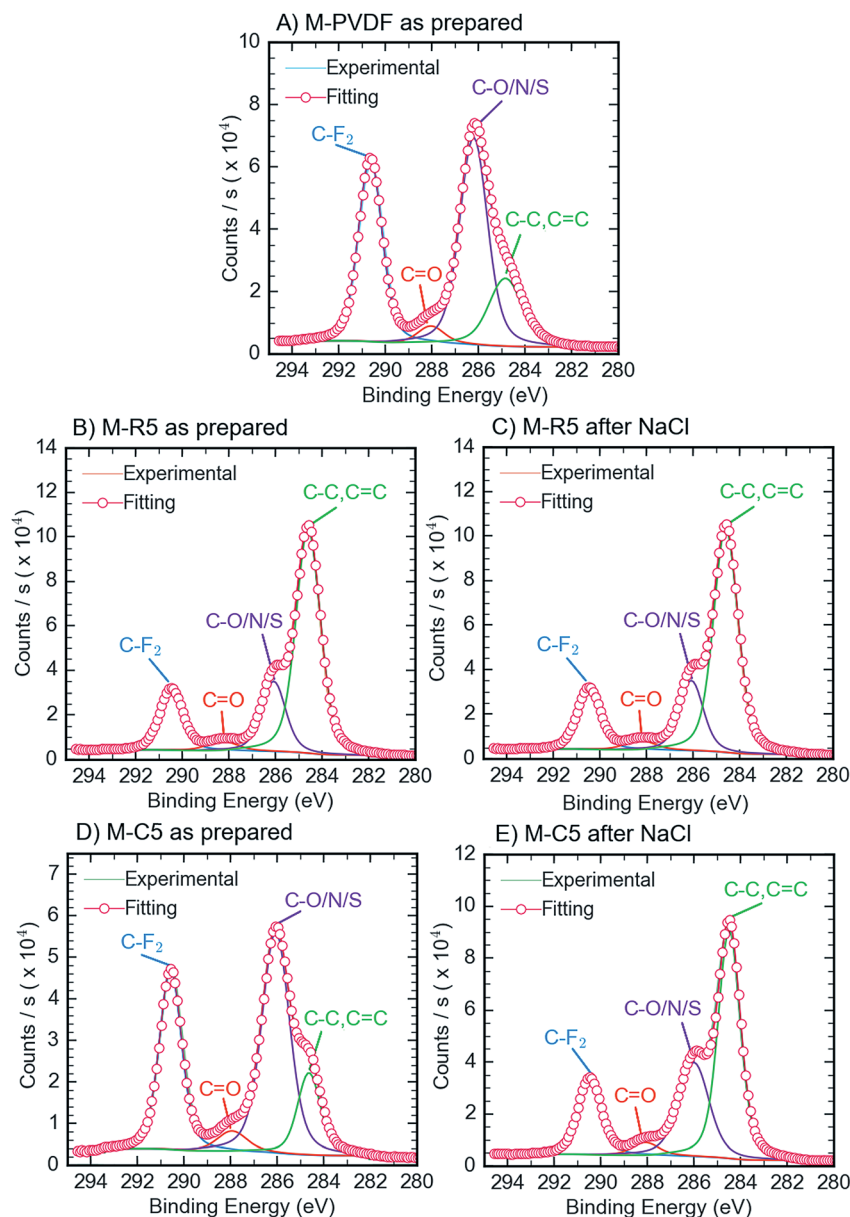


Fig. 7 Irreversible changes in the selective layer surface chemistry of membranes due to exposure to saline solutions, characterized by XPS high resolution C 1s spectra of (A) M-PVDF as prepared, (B) M-R5 as prepared, (C) M-R5 after immersion in 0.1 M NaCl, (D) M-C5 as prepared, and (E) M-C5 after immersion in 0.1 M NaCl.

Table 2 Atomic composition of membrane surfaces, acquired from XPS survey scans

Membrane code	Atomic%					C : F atomic ratio	(C-C, C=C, C-H) : (CF ₂) peak ratio
	C 1s	F 1s	O 1s	N 1s	S 2p		
M-PVDF as prepared	53.1	39.2	6.6	1.1	—	1.4	0.83
M-R5 as prepared	69.1	23.1	7.3	—	0.5	3.0	4.3
M-R5 after NaCl	76.1	14.8	8.6	—	0.6	5.2	7.6
M-C5 as prepared	53.4	38.2	6.2	1.7	0.6	1.4	0.45
M-C5 after NaCl	66.3	24.4	7.6	1.2	0.6	2.7	3.8

changes in the surface morphology and nanostructure. To test this hypothesis, we imaged the surface of M-R5 and M-C5 membranes using Atomic Force Microscopy (AFM) and

observed the surface topography before and after immersing each membrane in 0.1 M NaCl (Fig. 8). Before NaCl immersion, M-R5 ('M-R5 as prepared' in Fig. 8) had a relatively smooth

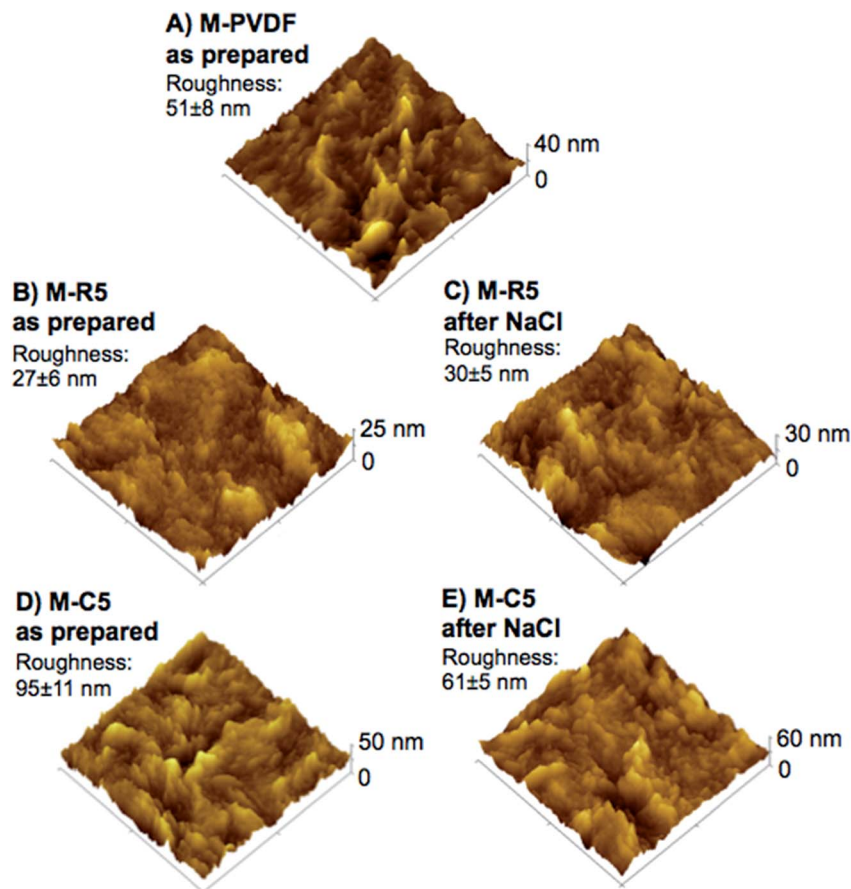


Fig. 8 AFM images from $10 \times 10 \mu\text{m}^2$ surface sections and measured surface roughness values of (A) M-PVDF as prepared, (B) M-R5 as prepared, (C) M-R5 after immersion in 0.1 M NaCl, (D) M-C5 as prepared, and (E) M-C5 after immersion in 0.1 M NaCl.

surface with broad, round features (RMS roughness = 27 ± 6 nm) compared to M-PVDF before NaCl immersion ('M-PVDF as prepared' in Fig. 8), which displayed rather narrow and pointed features (RMS roughness = 51 ± 8 nm). There was no significant change observed in the surface morphology or roughness of M-R5 upon exposure to salt ions ('M-R5 after NaCl' in Fig. 8), in agreement with the relatively minor changes in permeance. On the other hand, the surface of M-C5 before NaCl immersion ('M-C5 as prepared' in Fig. 8) featured broad but larger peaks, creating a significantly rougher surface (RMS roughness = 95 ± 11 nm). Interestingly, exposure to salt solution induced a smoothening effect on the surface of M-C5 ('M-C5 after NaCl' in Fig. 8), where the measured RMS roughness decreased to 61 ± 5 nm. This was another indication of ionic strength responsive reorganization in the surface nanostructure.

These results all indicate that exposure to saline aqueous solutions leads to significant, irreversible changes in membranes prepared from blends of PVDF with zwitterionic copolymers. These changes are much more prominent with the comb-shaped copolymer, in agreement with a few recent studies that demonstrated inter-chain bonding in dense brushes. These changes may also lead to variations in membrane fouling resistance.

3.5. Resistance to fouling by oil/water emulsions

The hydrocarbon processing industry, including petroleum refining, petrochemical processing and oil and natural gas production, produce extensive quantities of saline wastewater that include high contents of oil.⁹⁷ Fouling resistant membranes that can operate effectively in the presence of a complex mixture of salts, surfactants and oils would be remarkably beneficial for the reclamation of these streams. In this study, we prepared a representative saline oily water emulsion with a surfactant to initially test the robustness and fouling resistance of our membranes in a simulated oily feed stream. Since our results indicated that exposure to saline solutions increased the concentration of fouling resistant SB2VP groups on the membrane surface, we first equilibrated the membranes with a 0.1 M NaCl solution. This also resulted in the stabilization of the membrane permeance (see Fig. 6). Then, we filtered the oil/water emulsion prepared in 0.1 M NaCl for 24 hours. Finally, we rinsed the membrane and cell with 0.1 M NaCl, and measured the flux of this saline solution to determine the reversibility of any fouling.

The change in normalized flux, defined as the ratio of flux divided by the flux of 0.1 M NaCl upon equilibration, with time is shown in Fig. 9 for M-PVDF, M-R5 and M-C5 membranes. The non-normalized flux data with time are also plotted in Fig. S5,

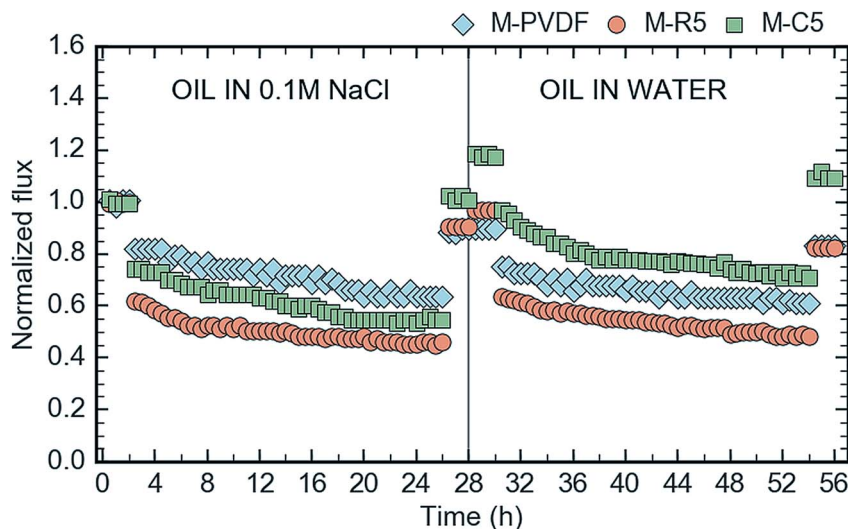


Fig. 9 Long-term oil fouling resistance by filtration of M-PVDF (10 psi), M-R5 (5 psi), and M-C5 (10 psi) membranes. The fluxes are plotted after normalizing by the average initial flux of each membrane: $19 \text{ L m}^{-2} \text{ h}^{-1}$ for M-PVDF, $38 \text{ L m}^{-2} \text{ h}^{-1}$ for M-R5, and $37 \text{ L m}^{-2} \text{ h}^{-1}$ for M-C5.

ESI.† It should be noted that, for a fair comparison, the filtration pressure was adjusted to achieve similar initial fluxes in testing M-R5 (5 psi) and M-C5 (10 psi) membranes. Despite its lower flux, M-PVDF filtrations were still conducted at 10 psi because of tearing observed toward the end of the second fouling cycle at higher pressures that would be required to match the initial flux of the other membranes.

The flux through all membranes declined upon exposure to the oily salt water. By the end of the first 24 hour fouling cycle with the oil-in-salt water emulsion, the flux of the M-R5 and M-C5 membranes declined to 46% and 55% of their initial salt water flux, respectively. The flux of M-PVDF declined to 64% of its initial flux. While this percentage decrease was somewhat less prominent than that observed for the membranes containing zwitterionic copolymers, we should mention that this membrane had to be operated at a lower initial flux ($19 \text{ L m}^{-2} \text{ h}^{-1}$ for M-PVDF), about half that of the additive containing membranes ($38 \text{ L m}^{-2} \text{ h}^{-1}$ for M-R5 and $37 \text{ L m}^{-2} \text{ h}^{-1}$ for M-C5). The initial water permeance of this membrane was about one fifth that of the M-R5 and M-C5 membranes. While we increased the trans-membrane pressure to enable a higher initial water flux, this was limited by the burst pressure of the membrane. The lower flux used throughout the fouling experiment meant that the hydrodynamic forces driving the oil droplets to the membrane surface were less significant in comparison with the shear force due to stirring.

Once the feed was switched back to 0.1 M NaCl, the M-C5 membrane fully recovered its initial flux, whereas the M-R5 and M-PVDF membranes both lost $\sim 10\%$ of their initial flux permanently due to irreversible oil fouling. The M-PVDF membrane showed the poorest performance, because it was fouled despite the lower amount of oily water filtered (130 mL) through the membrane during this cycle compared with the additive containing membranes (190 mL and 220 mL for M-R5 and M-C5, respectively).

After this experiment, we aimed to compare the fouling resistance of this equilibrated system to oil fouling in the absence of salts. While many of the changes observed in membrane surface chemistry were irreversible, some changes did occur upon switching back to deionized water. This means that feed ionic strength may affect interactions between the membrane surface and water, and also interactions between the membrane surface and oil droplets. To analyze this, we performed another fouling cycle where we conducted the same steps as above, but using deionized water instead of 0.1 M NaCl to prepare the oil emulsion. These data are also shown in Fig. 9, with a vertical line separating the two cycles.

During this second cycle, deionized water was filtered through the membranes first. This led to an 18% increase in the permeance of the M-C5 membrane due to the partial reversibility of ionic strength responsive permeance, in agreement with previous results (Fig. 6). The permeance of M-R5 also increased slightly, by 7% with respect to its flux after fouling. The permeance of M-PVDF remained unchanged, as expected. At the end of oil-in-water emulsion filtration, the best performance was again observed with the M-C5 membrane, which recovered 94% of its flux upon changing to a pure water feed. On the other hand, M-PVDF and M-R5 membranes both showed a $\sim 17\%$ permanent decline in their flux. Complete turbidity removal was achieved with all three membranes in both cycles, consistent with the typical performance of UF membranes with comparable MWCO values. The membrane prepared with the comb copolymer exhibits complete resistance to irreversible fouling when the aqueous feed is saline, whereas partial fouling is observed when the feed is of lower ionic strength. This is consistent with other studies that indicate that the hydrophilicity and fouling resistance of zwitterionic groups increase with ionic strength due to the anti-polyelectrolyte effect. A similar change is observed for the membrane containing the random copolymer, but this membrane shows minimal yet measurable

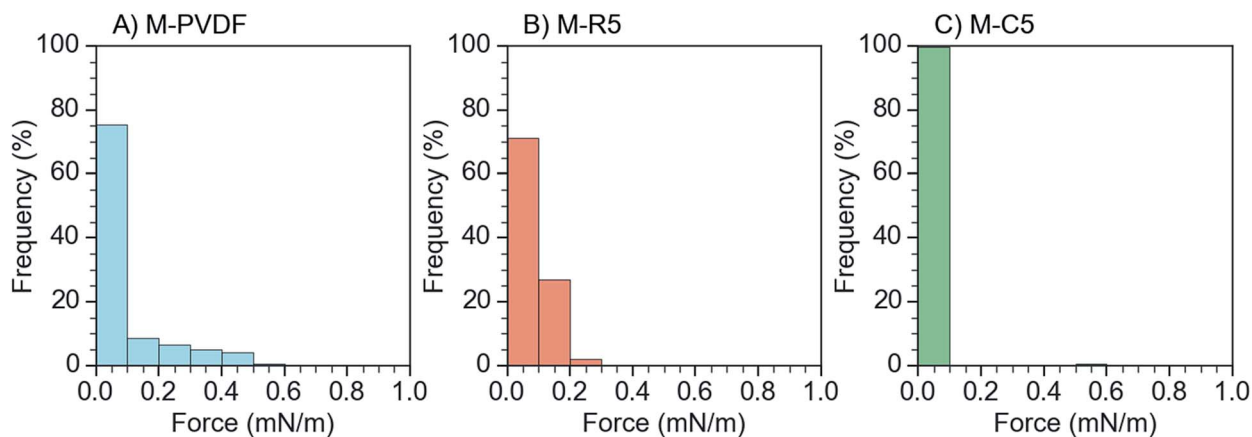


Fig. 10 Distributions of normalized jump-to-force measurements between the AFM particle (foulant) probe and membranes (A) M-PVDF, (B) M-R5, and (C) M-C5.

fouling even with a saline solution. Overall, our findings demonstrate that PVDF membranes incorporating the comb-shaped zwitterionic copolymer additive exhibit superior resistance to oil fouling in saline environments and sustain throughout the experiment in pure water.

3.6. Organic fouling propensity by AFM jump-to-force measurements

To better understand the fundamental mechanisms underlying the fouling resistance of zwitterionic membranes and to expand our findings to a wider range of organic foulants, we conducted AFM force measurements. Specifically, we measured the jump-to-force between a carboxylate modified latex particle probe, which represents common organic foulants, and the membrane surfaces. These measurements were conducted in phosphate buffered saline (PBS) to be consistent with previous organic fouling studies, which mostly employed protein foulants in PBS.^{40,98} To this end, jump-to-force measurements were performed for each of M-PVDF, M-R5 and M-C5 membranes (Fig. 10). The smallest jump-to-force was observed with the M-C5 membrane, where the attraction force values measured at all points on the membrane were below 0.1 mN m^{-1} . The jump-to-force values were somewhat higher for M-R5, and even higher for M-PVDF. These results were consistent with the detachment forces (Fig. S6, ESI†).

These results correlate well with our previously presented dynamic oil fouling results, which indicates that these AFM measurements may be used to predict membrane formulations that will exhibit higher fouling resistance. However, the oil emulsions used in previous experiments did not necessarily have negatively charged surfaces. To further support these findings, we also performed dynamic protein fouling tests with 24 h dead-end filtration of 1 g L^{-1} BSA solution in PBS as the foulant feed. Fouling resistance observed in the dead-end BSA filtration (Fig. S7, ESI†) was ultimately in agreement with jump-to-force measurements. The M-C5 membrane could retain 90% of its initial flux after 24 h of protein filtration, whereas M-R5 and M-PVDF membranes showed 15% and 18% irreversible flux

decline, respectively. The amount of BSA solution filtered through the control M-PVDF membrane (82 mL) was much lower than the amount filtered through the zwitterion-containing membranes (214 mL and 220 mL for M-R5 and M-C5, respectively). Overall, these results also confirmed that the comb copolymer additive provides stronger fouling resistance to the PVDF membrane in saline environments, likely due to better surface coverage, consistent with its surface segregation in saline environments shown by our surface analyses.

4. Conclusions

The use of designed copolymers as additives in membrane manufacture is simple and scalable, and thus provides a crucial tool for creating functional membranes for commercial use. Feeds with high ionic strength are common in many filtration feed streams, particularly in fracking wastewater, desalination and biotech applications. In this regard, membranes that perform particularly well at high ionic strengths can be advantageous. Furthermore, the use of a simple, easy to manipulate parameter such as ionic strength to impart irreversible changes in the membrane surface chemistry and morphology may enable the tuning of membrane performance for particular applications even after the manufacturing process is complete. The irreversible pore narrowing in response to salinity increase can be beneficial for the treatment of saline wastewater, especially produced and fracking water streams from oil and gas production.⁹⁹ The composition of these streams can vary substantially with location and throughout the life span of the well.¹⁰⁰ Salinity increase could well be correlated with rising complexity in these wastewater streams, considering all the polycyclic aromatic hydrocarbons (PAH), phenols, and traces of chemical additives used in drilling and fracking.^{100,101} Thus, permanent pore narrowing in response to salinity increase can be employed as a valve that enhances the membrane selectivity on demand and maintains the quality of otherwise compromised effluent due to potential smaller contaminants.

In this paper, we have blended PVDF with zwitterionic copolymers to manufacture fouling-resistant ultrafiltration

membranes. To determine the impact of the skeletal architecture of zwitterionic additives on the resulting membrane properties, we compared zwitterionic copolymers featuring two different architectural structures, random and comb-shaped. We synthesized the random copolymer PMMA-*r*-SB2VP using free radical polymerization, and the comb-shaped copolymer PVDF-*g*-SB2VP using ARGET-ATRP. Membranes were formed by blending up to 5 wt% zwitterionic copolymer with PVDF. The most competitive results were achieved with 5 wt% additive content. Our analysis showed that the water permeance increased to nearly five times that of pure PVDF membranes with the use of only 5 wt% of either additive. Interestingly, the membranes prepared with the comb copolymer additive exhibited irreversible changes in their permeance, surface chemistry and surface morphology upon exposure to saline water. The near-surface composition of this membrane became more significantly enriched in zwitterionic groups, and the surface nanostructure shifted to a smoother topology. In addition, the permeance of the comb copolymer containing membrane showed a sharp, permanent decline with increasing salt concentration in the feed. In contrast, the changes in the random copolymer containing membrane were relatively minor and mostly reversible. This difference in the ionic strength response between the random and comb additives was associated with increased spatial mobility of the zwitterionic groups in the comb architecture, allowing easier rearrangement of the zwitterionic groups in response to salinity. The comb additive containing membrane also showed better resistance against oil fouling and protein adhesion. In short, the use of a zwitterionic comb copolymer additive in the manufacture of PVDF membranes can lead to interesting new functionality, improved surface segregation in saline environments and promising fouling resistance.

Conflicts of interest

There are no conflicts to declare.

Acknowledgements

The authors gratefully acknowledge financial support from the National Science Foundation (NSF) under Grants No. CBET-1437772 and CHE-1508049. The authors thank Dr David Wilbur for assistance with NMR data collection and analysis, Prof. Qiaobing Xu for access to dynamic light scattering (DLS) and Atomic Force Microscopy (AFM) equipment, Dr Ilin Sadeghi for help with protein rejection measurements, Methira Saksir-iwatekul for experimental help with DLS measurements, and Prof. Zeynep Culfaz-Emecen and Begum Akean for useful discussions about protein fouling and potential applications. X-ray photoelectron spectroscopy (XPS) was conducted at Harvard University at the Center for Nanoscale Systems (CNS), a member of the National Nanotechnology Infrastructure Network (NNIN), supported by the National Science Foundation under NSF Award No. ECS-0335765. The authors thank Hao-Yu Greg Lin at the CNS for XPS training and assistance with data acquisition.

Notes and references

- I. Sadeghi, P. Kaner and A. Asatekin, *Chem. Mater.*, 2018, **30**, 7328–7354.
- A. Asatekin and C. Vannucci, *Nanosci. Nanotechnol. Lett.*, 2015, **7**, 21–32.
- H. B. Park, J. Kamcev, L. M. Robeson, M. Elimelech and B. D. Freeman, *Science*, 2017, 356.
- J. R. Werber, C. O. Osuji and M. Elimelech, *Nat. Rev. Mater.*, 2016, **1**, 16018.
- R. Zhang, Y. Liu, M. He, Y. Su, X. Zhao, M. Elimelech and Z. Jiang, *Chem. Soc. Rev.*, 2016, **45**, 5888–5924.
- W. S. Guo, H. H. Ngo and J. X. Li, *Bioresour. Technol.*, 2012, **122**, 27–34.
- M. F. A. Goosen, S. S. Sablani, H. Ai-Hinai, S. Ai-Obeidani, R. Al-Belushi and D. Jackson, *Sep. Sci. Technol.*, 2004, **39**, 2261–2297.
- N. Hilal, O. O. Ogunbiyi, N. J. Miles and R. Nigmatullin, *Sep. Sci. Technol.*, 2005, **40**, 1957–2005.
- H. C. Flemming, G. Schaule, T. Griebel, J. Schmitt and A. Tamachkiorowa, *Desalination*, 1997, **113**, 215–225.
- I. C. Escobar, E. M. Hoek, C. J. Gabelich, F. A. DiGiano, Y. A. Le Guellec, P. Berube, K. J. Howe, J. Allen, K. Z. Atasi, M. M. Benjamin, P. J. Brandhuber, J. Brant, Y. J. Chang, M. Chapman, A. Childress, W. J. Conlon, T. H. Cooke, I. A. Crossley, G. F. Crozes, P. M. Huck, S. N. Kommineni, J. G. Jacangelo, A. A. Karimi, J. H. Kim, D. F. Lawler, Q. L. Li, L. C. Schideman, S. Sethi, J. E. Tobiasson, T. Tseng, S. Veerapanemi, A. K. Zander and A. M. T. R. Comm, *Am. Water Works Assoc., J.*, 2005, **97**, 79–89.
- A. G. Fane and C. J. D. Fell, *Desalination*, 1987, **62**, 117–136.
- R. R. Choudhury, J. M. Gohil, S. Mohanty and S. K. Nayak, *J. Mater. Chem. A*, 2018, **6**, 313–333.
- R. E. Holmlin, X. X. Chen, R. G. Chapman, S. Takayama and G. M. Whitesides, *Langmuir*, 2001, **17**, 2841–2850.
- E. Ostuni, R. G. Chapman, R. E. Holmlin, S. Takayama and G. M. Whitesides, *Langmuir*, 2001, **17**, 5605–5620.
- I. Banerjee, R. C. Pangule and R. S. Kane, *Adv. Mater.*, 2011, **23**, 690–718.
- S. Colak and G. N. Tew, *Biomacromolecules*, 2012, **13**, 1233–1239.
- H. Kitano, A. Kawasaki, H. Kawasaki and S. Morokoshi, *J. Colloid Interface Sci.*, 2005, **282**, 340–348.
- E. Ostuni, R. G. Chapman, M. N. Liang, G. Meluleni, G. Pier, D. E. Ingber and G. M. Whitesides, *Langmuir*, 2001, **17**, 6336–6343.
- G. S. Georgiev, E. B. Karnenska, E. D. Vassileva, I. P. Kamenova, V. T. Georgieva, S. B. Iliev and I. A. Ivanov, *Biomacromolecules*, 2006, **7**, 1329–1334.
- J. F. Jhong, A. Venault, C. C. Hou, S. H. Chen, T. C. Wei, J. Zheng, J. Huang and Y. Chang, *ACS Appl. Mater. Interfaces*, 2013, **5**, 6732–6742.
- M.-Z. Li, J.-H. Li, X.-S. Shao, J. Miao, J.-B. Wang, Q.-Q. Zhang and X.-P. Xu, *J. Membr. Sci.*, 2012, **405–406**, 141–148.
- Q. Li, Q. Y. Bi, B. Zhou and X. L. Wang, *Appl. Surf. Sci.*, 2012, **258**, 4707–4717.

- 23 Q. Li, B. Zhou, Q.-Y. Bi and X.-L. Wang, *J. Appl. Polym. Sci.*, 2012, **125**, 4015–4027.
- 24 Y. Liu, S. L. Zhang and G. B. Wang, *Desalination*, 2013, **316**, 127–136.
- 25 W. W. Yue, H. J. Li, T. Xiang, H. Qin, S. D. Sun and C. S. Zhao, *J. Membr. Sci.*, 2013, **446**, 79–91.
- 26 G. Q. Zhai, S. C. Toh, K. L. Tan, E. T. Kang, K. G. Neoh, C. C. Huang and D. J. Liaw, *Langmuir*, 2003, **19**, 7030–7037.
- 27 Y.-H. Zhao, K.-H. Wee and R. Bai, *ACS Appl. Mater. Interfaces*, 2009, **2**, 203–211.
- 28 R. Yang, J. J. Xu, G. Ozyaydin-Ince, S. Y. Wong and K. K. Gleason, *Chem. Mater.*, 2011, **23**, 1263–1272.
- 29 R. Yang and K. K. Gleason, *Langmuir*, 2012, **28**, 12266–12274.
- 30 R. Yang, A. Asatekin and K. K. Gleason, *Soft Matter*, 2012, **8**, 31–43.
- 31 F.-N. Meng, M.-Q. Zhang, K. Ding, T. Zhang and Y.-K. Gong, *J. Mater. Chem. A*, 2018, **6**, 3231–3241.
- 32 Q. Sun, Y. L. Su, X. L. Ma, Y. Q. Wang and Z. Y. Jiang, *J. Membr. Sci.*, 2006, **285**, 299–305.
- 33 Y. L. Su, L. L. Zheng, C. Li and Z. Y. Jiang, *J. Phys. Chem. B*, 2008, **112**, 11923–11928.
- 34 L. J. Wang, Y. L. Su, L. L. Zheng, W. J. Chen and Z. Y. Jiang, *J. Membr. Sci.*, 2009, **340**, 164–170.
- 35 S. Rajabzadeh, D. Ogawa, Y. Ohmukai, Z. Zhou, T. Ishigami and H. Matsuyama, *Desalin. Water Treat.*, 2015, **54**, 2911–2919.
- 36 K. Tu, P. Shen, J. Li, B. Fan, C. Yang and R. Du, *J. Appl. Polym. Sci.*, 2015, **132**, 41362.
- 37 X. J. Huang, Z. K. Xu, L. S. Wan, Z. G. Wang and J. L. Wang, *Macromol. Biosci.*, 2005, **5**, 322–330.
- 38 Z. Yi, L.-P. Zhu, H. Zhang, B.-K. Zhu and Y.-Y. Xu, *Polymer*, 2014, **55**, 2688–2696.
- 39 X. Zhao, W. Chen, Y. Su, W. Zhu, J. Peng, Z. Jiang, L. Kong, Y. Li and J. Liu, *J. Membr. Sci.*, 2013, **441**, 93–101.
- 40 P. Kaner, E. Rubakh, D. H. Kim and A. Asatekin, *J. Membr. Sci.*, 2017, **533**, 141–159.
- 41 S. Kang, A. Asatekin, A. M. Mayes and M. Elimelech, *J. Membr. Sci.*, 2007, **296**, 42–50.
- 42 A. Asatekin, S. Kang, M. Elimelech and A. M. Mayes, *J. Membr. Sci.*, 2007, **298**, 136–146.
- 43 X. W. Fan, L. J. Lin and P. B. Messersmith, *Biomacromolecules*, 2006, **7**, 2443–2448.
- 44 D. G. Walton and A. M. Mayes, *Phys. Rev. E*, 1996, **54**, 2811.
- 45 D. G. Walton, P. P. Soo, A. M. Mayes, S. J. S. Allgor, J. T. Fujii, L. G. Griffith, J. F. Ankner, H. Kaiser, J. Johansson, G. D. Smith, J. G. Barker and S. K. Satija, *Macromolecules*, 1997, **30**, 6947–6956.
- 46 A. Asatekin, S. Kang, M. Elimelech and A. M. Mayes, *J. Membr. Sci.*, 2007, **298**, 136–146.
- 47 A. Asatekin and A. M. Mayes, *Environ. Sci. Technol.*, 2009, **43**, 4487–4492.
- 48 R. Knoesel, M. Ehrmann and J. C. Galin, *Polymer*, 1993, **34**, 1925–1932.
- 49 G. S. Georgiev, E. B. Karnenska, E. D. Vassileva, I. P. Kamenova, V. T. Georgieva, S. B. Iliev and I. A. Ivanov, *Biomacromolecules*, 2006, **7**, 1329–1334.
- 50 A. B. Lowe and C. L. McCormick, *Chem. Rev.*, 2002, **102**, 4177–4190.
- 51 Q. Yang and M. Ulbricht, *Chem. Mater.*, 2012, **24**, 2943–2951.
- 52 G. Zhai, S. C. Toh, W. L. Tan, E. T. Kang, K. G. Neoh, C. C. Huang and D. J. Liaw, *Langmuir*, 2003, **19**, 7030–7037.
- 53 Y.-H. Zhao, K.-H. Wee and R. Bai, *ACS Appl. Mater. Interfaces*, 2009, **2**, 203–211.
- 54 J. Choi and M. F. Rubner, *Macromolecules*, 2005, **38**, 116–124.
- 55 W. A. Phillip, R. Mika Dorin, J. r. Werner, E. M. V. Hoek, U. Wiesner and M. Elimelech, *Nano Lett.*, 2011, **11**, 2892–2900.
- 56 C. Geismann, F. Tomicki and M. Ulbricht, *Sep. Sci. Technol.*, 2009, **44**, 3312–3329.
- 57 Y. Cho, J. Lim and K. Char, *Soft Matter*, 2012, **8**, 10271–10278.
- 58 Q. Shi, Y. Su, X. Ning, W. Chen, J. Peng and Z. Jiang, *J. Membr. Sci.*, 2010, **347**, 62–68.
- 59 H. H. Himstedt, K. M. Marshall and S. R. Wickramasinghe, *J. Membr. Sci.*, 2011, **366**, 373–381.
- 60 L. Ying, E. Kang, K. Neoh, K. Kato and H. Iwata, *J. Membr. Sci.*, 2004, **243**, 253–262.
- 61 A. Nykänen, M. Nuopponen, A. Laukkanen, S.-P. Hirvonen, M. Rytelä, O. Turunen, H. Tenhu, R. Mezzenga, O. Ikkala and J. Ruokolainen, *Macromolecules*, 2007, **40**, 5827–5834.
- 62 K. Dutta and S. De, *J. Mater. Chem. A*, 2017, **5**, 22095–22112.
- 63 M. Annaka and T. Tanaka, *Nature*, 1992, **355**, 430.
- 64 K. Itano, J. Choi and M. F. Rubner, *Macromolecules*, 2005, **38**, 3450–3460.
- 65 K. E. Secrist and A. J. Nolte, *Macromolecules*, 2011, **44**, 2859–2865.
- 66 D. Lee, A. J. Nolte, A. L. Kunz, M. F. Rubner and R. E. Cohen, *J. Am. Chem. Soc.*, 2006, **128**, 8521–8529.
- 67 J. A. Hiller and M. F. Rubner, *Macromolecules*, 2003, **36**, 4078–4083.
- 68 T. Xiang, M. Tang, Y. Liu, H. Li, L. Li, W. Cao, S. Sun and C. Zhao, *Desalination*, 2012, **295**, 26–34.
- 69 J. L. Weidman, R. A. Mulvanna, B. W. Boudouris and W. A. Phillip, *J. Am. Chem. Soc.*, 2016, **138**, 7030–7039.
- 70 B. Jeong, C. F. Windisch, M. J. Park, Y. S. Sohn, A. Gutowska and K. Char, *J. Phys. Chem. B*, 2003, **107**, 10032–10039.
- 71 H. Cheng, L. Shen and C. Wu, *Macromolecules*, 2006, **39**, 2325–2329.
- 72 J. F. Hester, P. Banerjee and A. M. Mayes, *Macromolecules*, 1999, **32**, 1643–1650.
- 73 J.-H. Li, M.-Z. Li, J. Miao, J.-B. Wang, X.-S. Shao and Q.-Q. Zhang, *Appl. Surf. Sci.*, 2012, **258**, 6398–6405.
- 74 C. Vannucci, I. Taniguchi and A. Asatekin, *ACS Macro Lett.*, 2015, **4**, 872–878.
- 75 S. Mori and H. G. Barth, *Size Exclusion Chromatography*, Springer, Heidelberg, Germany, 2013.
- 76 J. F. Jhong, A. Venault, C. C. Hou, S. H. Chen, T. C. Wei, J. Zheng, J. Huang and Y. Chang, *ACS Appl. Mater. Interfaces*, 2013, **5**, 6732–6742.
- 77 M.-Z. Li, J.-H. Li, X.-S. Shao, J. Miao, J.-B. Wang, Q.-Q. Zhang and X.-P. Xu, *J. Membr. Sci.*, 2012, **405**, 141–148.

- 78 Q. Li, Q.-Y. Bi, T.-Y. Liu and X.-L. Wang, *Appl. Surf. Sci.*, 2012, **258**, 7480–7489.
- 79 Q. Li, B. Zhou, Q.-Y. Bi and X.-L. Wang, *J. Appl. Polym. Sci.*, 2012, **125**, 4015–4027.
- 80 Q. Li, J. Imbrogno, G. Belfort and X. L. Wang, *J. Appl. Polym. Sci.*, 2015, **132**, 41781.
- 81 Y. Zhu, F. Zhang, D. Wang, X. F. Pei, W. Zhang and J. Jin, *J. Mater. Chem. A*, 2013, **1**, 5758–5765.
- 82 R. Yang, J. J. Xu, G. Ozaydin-Ince, S. Y. Wong and K. K. Gleason, *Chem. Mater.*, 2011, **23**, 1263–1272.
- 83 K. Kratz, W. Xie, A. Lee, B. D. Freeman and T. Emrick, *Macromol. Mater. Eng.*, 2011, **296**, 1142–1148.
- 84 P. Kaner, D. J. Johnson, E. Seker, N. Hilal and S. A. Altinkaya, *J. Membr. Sci.*, 2015, **493**, 807–819.
- 85 I. Sadeghi, H. Yi and A. Asatekin, *Chem. Mater.*, 2018, **30**, 1265–1276.
- 86 P. Prentice, *Polymer*, 1983, **24**, 344–350.
- 87 P. Bengani-Lutz, E. Converse, P. Cebe and A. Asatekin, *ACS Appl. Mater. Interfaces*, 2017, **9**, 20859–20872.
- 88 Q. Shao, Y. He, A. D. White and S. Jiang, *J. Phys. Chem. B*, 2010, **114**, 16625–16631.
- 89 Q. Shao and S. Jiang, *Adv. Mater.*, 2015, **27**, 15–26.
- 90 J. F. Hester, P. Banerjee, Y. Y. Won, A. Akthakul, M. H. Acar and A. M. Mayes, *Macromolecules*, 2002, **35**, 7652–7661.
- 91 P. Kaner, P. Bengani-Lutz, I. Sadeghi and A. Asatekin, *Technology*, 2016, **4**, 217–228.
- 92 D. Wandera, S. R. Wickramasinghe and S. M. Husson, *J. Membr. Sci.*, 2010, **357**, 6–35.
- 93 G. S. Georgiev, E. B. Kamenska, E. D. Vassileva, I. P. Kamenova, V. T. Georgieva, S. B. Iliev and I. a. Ivanov, *Biomacromolecules*, 2006, **7**, 1329–1334.
- 94 J. B. Schlenoff, *Langmuir*, 2014, **30**, 9625–9636.
- 95 G. Beamson and D. Briggs, *High Resolution XPS of Organic Polymers: the Scienta ESCA300 Database*, Wiley, Chichester, England, 1992.
- 96 G. P. López, D. G. Castner and B. D. Ratner, *Surf. Interface Anal.*, 1991, **17**, 267–272.
- 97 M. Cheryan and N. Rajagopalan, *J. Membr. Sci.*, 1998, **151**, 13–28.
- 98 P. Kaner, X. Hu, S. W. Thomas and A. Asatekin, *ACS Appl. Mater. Interfaces*, 2017, **9**, 13619–13631.
- 99 A. Zaidi, K. Simms and S. Kok, *Water Sci. Technol.*, 1992, **25**, 163–176.
- 100 L.-G. Faksness, P. G. Grini and P. S. Daling, *Mar. Pollut. Bull.*, 2004, **48**, 731–742.
- 101 B. A. Farnand and T. A. Krug, *J. Can. Pet. Technol.*, 1989, **28**, 18–26.